Version of Record: https://www.sciencedirect.com/science/article/pii/S156753942200295X
Manuscript_8459d5e9679d8180ed99eea9c9e2a82d

Electrochemical monitoring of the *Pseudomonas aeruginosa* growth and the formation of a biofilm in TSB media

J. Pellé[a], M. Longo[a,b*], N. Le Poul[c], C. Hellio[b], S. Rioual[a], B. Lescop[a],

[a] Univ Brest, Lab-STICC, CNRS, UMR 6285, F-29200 Brest, France

[b] Univ Brest, BIODIMAR/LEMAR, CNRS, UMR 6539, F-29200, Brest, France

[c] Univ Brest, CEMCA, CNRS, UMR 6521, F-29200, Brest, France

* Co-first author

Abstract:

Understanding and sensing microbial biofilm formation onto surfaces remains highly challenging for preventing corrosion and biofouling processes. For that purpose, we have thoroughly investigated biofilm formation onto glassy carbon electrode surfaces by using electrochemical technics. *Pseudomonas aeruginosa* was studied because of its remarkable ability to form biofilms in many environments. The modification of the electrode-solution interface during biofilm growth was monitored by *in-situ* measurement of the open-circuit potential and correlated with results obtained by electrochemical impedance spectroscopy, cyclic voltammetry, scanning electron microscopy and bioassays. The sensing of the biofilm formation hence suggests a multi-steps mechanism, which may include pre-formation of an insulating layer onto the surface prior to the bacteria adhesion and biofilm formation.

Keywords: *Pseudomonas aeruginosa*, biofilm formation, open-circuit potential, electrochemical impedance spectroscopy, cyclic voltammetry

1. Introduction

Microbial biofilm formation is a significant issue for marine industries. Indeed, it leads to the microbiologically influenced corrosion (MIC) which increases significantly the rate of corrosion of marine immersed structures, such as ships hulls or marine energy devices [1], and is responsible for biofouling that can increase considerably the weight of structures [2]. Within this context, low cost and efficient devices, which can assess both bacterial growth and biofilm formation, are urgently needed. Many techniques, mainly based on fluorescence and mass spectrometry, have been developed for this purpose [3-7]. However, they solely allow *ex situ* characterization of biofilm and do not match with the need of an *in situ* and real time monitoring of the biofilm formation [8]. Examples of direct measurements by using optical microscopy techniques such as SEM or confocal laser scanning have been reported [9]. However, these techniques are usually expensive, they need preparation and sometimes specific chemicals such as fluorophores. In comparison, electrochemical sensors appear as the best candidates for real time monitoring of biofilms [10], due to their short response time, easy manufacture, low-cost, high sensitivity and possibility of miniaturization [11, 12]. So far, lots of electrochemical studies on biofilms have focused on the variation of the open circuit potential (E_{OC}) versus time in order to monitor the film growth, which represents a common tool for the biofilm monitoring on steels [13]. However, electrochemical impedance spectroscopy (EIS) has gained attention in biofilm research for its ability to detect slight changes at electrode/electrolyte interface associated to the adhesion of bacteria cells on the electrode [14]. This information on the interfacial properties can be converted in terms of equivalent circuits including capacitances and resistances.

The bacterial activity was investigated for steels surfaces [15-18], revealing a decrease of E_{OC} with time upon biofilm formation. This negative shift of the open circuit potential was correlated to the increase of bacterial concentration [16-18]. In addition, EIS studies demonstrated that the global charge transfer resistance of the electrode could be decreased upon biofilm growth [18]. Although these electrochemical studies have provided general trends, detailed explanations of the phenomena are still difficult to extract due to possible change of steel's passivation with biofilm formation. Moreover, correlation between bacteria growth and biofilm formation is still unclear from most of the electrochemical studies previously mentioned. Based on these statements, it is obvious that there is a need to provide model systems which can allow further and clear interpretation of biofilm growth. Using materials which can be considered as "chemically inert" (i.e. not reactive towards chemicals)

such as glassy carbon (GC) instead of steel is a strategy which has been only recently reported for that purpose. Poma *et al.* [19] monitored the variation of E_{OC} on functionalized reduced graphene oxide electrodes during the growth of three bacteria. As for steel, a decrease of the open circuit potential was found during bacterial growth. However, no clear ratio was established between the relative open circuit value and the bacteria concentration. Nevertheless, their experiment was stopped after 6 hours and no biofilm formation could be experimentally evidenced.

In this context, the herein study describes a thorough investigation of the bacterial colonization and biofilm formation onto a GC electrode over days in culture media of *P. aeruginosa,* which is well known to produce biofilm in a short amount of time compared to other bacterial species [20-22]. Based on our findings, we provided a new model for biofilm growth on inert surfaces. This work will serve as a strong basis for future comparative studies with less inert materials such as steel surfaces to fully decipher and possibly quantify the role of the surface in the adsorption events and biofilm growth. Electrochemical techniques (open-circuit potential monitoring, EIS and cyclic voltammetry (CV)) as well as scanning electron microscopy (SEM) were used to analyse the modified surfaces at the different stages of biofilm growth. These techniques were combined with biological assays to correlate bacterial concentration to biofilm formation. In particular, the use of EIS and CV techniques has allowed accurate determination of the interfacial properties during these processes.

2. Materials and methods

2.1. Microorganisms, preculture and cell growth

The gram-negative model bacteria *Pseudomonas aeruginosa* (Schroeter) (PA01) was selected for the study. It was inoculated from frozen stock into Teflon tube containing 50 mL of Tryptic Soy Broth (TSB) media. The strain was then incubated overnight at 37°C. For all the experiments, 150 µL of bacterial suspension was inoculated in 20 mL of TSB (about 1% v/v diluted). In order to determine kinetics of cells formation, the pre-culture was inoculated in 60 mL of TSB to reach a concentration of 2 x 10^7 CFU/mL for *P. aeruginosa*. Every 30 minutes during 48 h, 500 µL of medium was collected and the OD_{600} was measured with a spectrophotometer in 8 replicates (TECAN Infinite™). Kinetics of the biofilm formation were evaluated by labelling the biofilm with Crystal Violet in 96-well plates. Measurements were made every 2 hours during 48 hours. Using each time a single 96 wells plate. Among the 96

wells, 80 wells were used as replicates, while the 16 remaining were used as control. In each replicates, 15 µL of bacteria were inoculated in 200 µL of TSB culture solution. Then, all plates were incubated at 37°C during different times to complete the whole kinetic study. The labelling of adhered matter was performed by adding 50 µL of a Crystal Violet solution in each of the wells. After 10 minutes, the content of the wells was removed and a very delicate washing was performed by soaking the plates in a distilled water bath. Finally, 200 µL of ethanol was added to solubilize the stained adhered cells. The determination of the specific biofilm formation (SBF) values was calculated according to the method reported by Naves *et al*. [23].

2.2. Electrochemical measurements

2.2.1. Glassy carbon electrode preparation

The glassy carbon (GC) electrode (A = 0.071 cm^2) was purchased from CHI (CHI104 model). In order to obtain a homogeneous surface for each experiment, it was first polished on emery paper. After rinsing with water, it was further polished on an alumina (1 µm) cloth, rinsed with water, cleaned in an ultrasonic bath with distilled water, and dried with an air stream.

2.2.2. Experimental settings

A classical three-electrode configuration was used in all electrochemical experiments. The working electrode (WE) was a glassy carbon electrode. The counter electrode (CE) was a platinum wire. The reference electrode (RE) was an Ag/AgCl, KCl (3M) electrode (E = + 0.210 V *vs*. SHE at 25°C). Before each experiment, the WE was immersed in sterile TSB for 4h in order to stabilize the electrode potential. Electrochemical measurements (OCP monitoring, cyclic voltammetry and electrochemical impedance spectroscopy) were performed using either a SP200 (Bio-logic) potentiostat or a PGSTAT30 (Metrohm) apparatus. CV and EIS were performed in $[Fe(CN)_6]K_3$ (0.5 mM) / KCl (0.1 M) / H_2O. EIS measurements were carried out on a frequency range from 100 kHz to 10 mHz, with an amplitude of 10 mV to respect the linearity of the system. The applied potential was fixed at the half-wave potential $E_{1/2}$ determined from CV measurements in the ferricyanide solution.

2.2.3. *Scanning Electron Microscopy (SEM)*

The morphological analysis of bacteria and biofilm deposited on pieces of a GC electrode were carried out using SEM Hitachi – S800 microscope. For higher resolution, few drops of a solution of HILEM IL1000 were deposited on the samples.

3. Results and discussion

3.1. E_{OC} monitoring with bacterial growth

The measurements of open-circuit potential at the glassy carbon electrode were carried out at 37°C to account for kinetics of the process. Fig. 1 shows the variation of E_{OC} with time in TSB culture media. The bacteria concentration and the SBF index are also presented in Fig. 1. Four measurements of E_{OC} were performed in order to produce a mean curve with the standard deviation. Three stages can be observed and described as follows. From 0 to 1 hour (step 1), the potential variation is low (< 2 $mV.h^{-1}$). Then, a significant decrease (approx. 30 $mV.h^{-1}$) occurs until approx. 6 hours (step 2). Lastly, the open circuit potential slowly decreases (2 $mV.h^{-1}$) until the end of the test (step 3). The observed behaviour can be compared to the variation of the bacterial concentration and biofilm formation. Indeed, an overlay between electrochemical monitoring and biological measurements is depicted in Fig. 1. Step 1 is correlated to the latency phase observed in a classical cycle of bacteria growth [24]. This corresponds to the first moments of bacterial growth, when the division of bacteria has not reached the exponential phase yet. Then, the strong decrease in potential observed in step 2 is associated with the exponential planktonic growth. The maximum concentration is reached after 10 hours and does not evolve after. Lastly, the E_{OC} break obtained at 6 hours seems to correspond to the beginning of the biofilm formation. Moreover, the biofilm increase shows an ongoing growth over time to achieve a quasi-steady-state thickness after 30 hours (hence justifying long-period measurements).

Here Figure 1

To confirm these hypotheses, SEM studies were performed for different stages of the bacterial growth with GC electrode pieces. For SEM experiments, two immersion times were chosen in

stages 2 and 3. Fig 2 presents SEM images of GC surfaces immersed in inoculated TSB for 3 hours and 24 hours. The differences obtained between the two immersion times are striking. Indeed, after 3 hours of immersion, most of the surface is bacteria free (Fig. 2a). In contrast, after 24 hours of immersion, the number of bacteria present on the surface is much higher (Fig. 2b). Moreover, a matrix in which bacteria seem to be embedded is distinguished on the image, most likely the biofilm, similarly to what was observed by Wijesinghe *et al*. [25]. At the bacteria scale, the biofilm shows a significantly rough surface. Thus, these visual observations clearly highlight an evolution of the surface that corroborate with electrochemical and biological monitoring.

Here Figure 2

From electrochemical and microscopic measurements, the process chronology can be summarized as follows:

(i) An initiation/latency step for which E_{OC} is stable because the bacteria concentration is too low and no biofilm can be formed.

(ii) A significant decrease of E_{OC} when the bacteria concentration starts increasing, although no biofilm is necessarily formed. This may include the progressive adsorption / deposition of bacteria onto the electrode surface.

(iii) The bacteria concentration is at their maximum and biofilm is formed, the open-circuit potential shows a very slight decrease.

In order to further determine which parameters affect the formation of the biofilm on the inert electrode, we also varies the initial concentration of bacteria in the culture media and monitored E_{OC} values (see in SI). The results suggest that a threshold value of concentration exists below which the evolution of the open-circuit potential is independent of the bacterial concentration.

3.2. CV measurements

In addition to the open-circuit monitoring studies, CV and EIS measurements were carried out in order to better investigate the conducting properties of the electrode surface covered by a biofilm. For these two techniques, a well-known redox probe (ferricyanide) was used to afford direct determination / visualization of the electron transfer kinetics across the electrode / biofilm / solution interfaces. The results obtained by cyclic voltammetry are displayed in Fig. 3. When a bare GC electrode was used (black curve, Fig. 3), a quasi-reversible system corresponding to the ferri/ferro system was found as previously reported [26-28]

Here Figure 3

When the GC electrode was dipped in the culture media containing *P. aeruginosa* for 48 hours (after 4h of stabilization) then rinsed with ethanol and water (to avoid bacteria contamination and to fix the biofilm), the resulting CV in ferricyanide displayed no peak (blue curve, Fig. 3). This behavior is typical for an insulating layer which blocks the electron transfer to this inorganic probe [29], as found for instance with a covalently-bound organic layer [26]. That means the surface of the electrode has changed, which is consistent with the biofilm formation observed in Fig. 2. Hence, the layer of biofilm formed at the surface prevents the charge transfer. This is particularly unexpected since bacteria are known to be conductive species, as shown by Maruthupandy *et al.* [30] with electrochemical techniques (CV and EIS). However, some studies also found that there is a decrease of the conductivity inside the biofilm that could be due to the presence of polysaccharides, known for being insulating [31, 32].

To investigate the possible influence of the TSB media on the CV results of biofilm, a polished electrode was immersed in culture media for 4 hours without any bacteria. This immersion time was selected to simulate the equilibration time experimentally used: to do so, for all the experiments, bacteria were introduced into the solution after this stabilization time. CV obtained (red curve, Fig. 3) shows behavior redox different compared to bare GC. Clearly, this result indicates that despite the absence of bacteria in the solution, a strongly-adsorbed layer is deposited at short times, slowing down the electron transfer. During the equilibration time (about 4h), E_{OC} was measured and no significant change was reported. So, this adsorbed layer does not significantly affect the open-circuit potential. Further

experimentations (data not shown in this paper) have allowed to conclude that the tryptone from TSB triggers the adsorption process. Unfortunately, due to the large number of components of tryptone, it was not possible to decipher precisely the exact nature of the adsorbed species. Such an adsorbed layer, which has never been mentioned in the literature so far, has been then integrated to the new model proposed in this work.

3.3. EIS measurements

EIS measurements in ferricyanide were performed concomitantly to CV in order to better analyse electron transfer process in terms of capacitive and faradaic currents. Bare GC, GC after 4h in TSB and GC covered with a biofilm were studied. Experimental data are presented through classical Nyquist (Fig. 4) and Bode diagrams (see diagram in SI). The Nyquist plots were fitted according to an equivalent circuit including (i) the electrolyte resistance (R_e), (ii) the charge transfer resistance (R_{ct}) and double layer pseudo-capacitance (C_{dl}) for the ferri/ferrocyanide electron transfer, and (iii) two RC-like parallel components which account for the biofilm and the adsorbed layer suggested by CV experiments (Fig. 6). Table 1 gathers EIS data obtained from curve fitting (see fits in SI).

Here Figure 4

The Nyquist plots for the bare GC electrode (black curve, Fig. 4) display a capacitive loop for high frequencies (> 1 Hz) yielding R_{ct} = 0.65 kΩ.cm^2 and Q_{dl} = 40.6 µF.s$^{\alpha-1}$.cm^2. For lower frequencies, a linear variation with a 45° slope is obtained as expected for a mass-transfer controlled regime (Warburg diffusion). Such behavior is classical for a relatively fast charge-transfer process with no blocking layer, as found by CV.

Here Table 1

With the electrode immersed in sterile TSB for 4 hours, R_{ct} was found to increase up to 7.1 kΩ.cm^2. This result is consistent with the formation of a blocking layer as found by CV. When the electrode was dipped for 48 h in TSB with bacteria, the charge transfer resistance was found to increase even more (8.6 kΩ.cm^2). These results are fully in agreement with CV

and reinforce the hypothesis that an adsorbed and insulating layer is formed during the equilibrium stage in sterile TSB. Further insights into the EIS analysis allowed determination of the resistances and pseudo-capacitances for the biofilm and first-adsorbed layers according to the equivalent circuit shown in Fig. 5b.

Here Figure 5

Impedance values for the biofilm ($R_{biofilm}$, Table 1) indicate that the biofilm is clearly not conductive under these conditions. This is in accordance with the increase in biofilm resistance observed over time by Liu *et al.* [31], although the proposed model is simpler since it does not take account of the adsorbed layer. The insulating property is most likely due to the biofilm matrix, which contains polysaccharides as they are known for being insulating [31, 32].

Regarding the E_{OC} monitoring shown in Fig. 1, EIS data suggest that even in absence of bacteria (or below a critical concentration), the GC electrode – TSB electrolyte interface undergoes adsorption processes, without significantly affecting the open-circuit potential. When the bacteria concentration increases, the number of bacteria units adsorbed on the electrode also raises and induces a decrease of the open-circuit potential due possibly to the negatively charged phosphates and sulphates groups. Generation of a biofilm by the bacteria may decrease the global conductivity of the two layers, and also affect E_{OC} to finally reach a steady-state value for which the bacteria concentration, the biofilm thickness, the open-circuit potential and the conductive properties do not evolve (Schematic 1).

Here Schematic 1

4. Conclusion

This work aimed at providing new insights into the bacterial colonization and biofilm formation onto a GC surface using *P. aeruginosa* in TSB media. The *in-situ* open-circuit potential sensing combined to *ex-situ* EIS, CV and SEM have provided novel information on

the different processes occurring for the biofilm generation. While long-time *in-situ* measurements have clearly emphasized that E_{oc} could be not only correlated to the increase of bacteria concentration, CV and impedance experiments have demonstrated the possible formation of an insulating layer on the electrode prior to bacteria deposition and biofilm formation in TSB. These remarkable results open the discussion on the conditions required to favour biofilm formation. Indeed, control of bacteria concentration close to the electrode interface may avoid biofilm formation. Furthermore, the ad-layer formed from the culture media could be crucial for the further deposition of bacteria accompanied with a drop of the open-circuit potential. At last, the model proposed here could be further exploited for the analysis of steel surfaces.

Acknowledgements

This research was funded by Agence Nationale de la Recherche (France), grant number ANR-19-SARG-0006. This work is also supported by the European Union through the European Regional Development Fund (ERDF), the Ministry of Higher Education and Research, the Région Bretagne, Biogenouest, the Conseil Départemental du Finistère and Brest Métropole Océane, through the CPER Project 2015-2020 MATECOM.

References

[1] A. Farkas, N. Degiuli and I. Martić, Assessment of the effect of biofilm on the ship hydrodynamic performance by performance prediction method, Int. J. Nav. Archit. Ocean. Eng. 13 (2021) 102-114. https://doi.org/10.1016/j.ijnaoe.2020.12.005.

[2] V.J.D. Rascio, Antifouling coatings: where do we go from here, Corros. Rev. 18 (2000) 133-154. https://doi.org/10.1515/CORRREV.2000.18.2-3.133.

[3] S. Malic, K.E. Hill, A. Hayes, S.L. Percival, D.W. Thomas and D.W. Williams, Detection and identification of specific bacteria in wound biofilms using peptide nucleic acid fluorescent in situ hybridization (PNA FISH), Microbiology 155 (2009) 2603-2611. https://doi.org/10.1099/mic.0.028712-0

[4] C. Almeida, N.F. Azevedo, S. Santos, C.W. Keevil, M.J. Vieira, Discriminating multi-species populations in biofilms with peptide nucleic acid fluorescence in situ hybridization (PNA FISH), Plos One 6 (2011) e14786. https://doi.org/10.1371/journal.pone.0014786

[5] Y. Song, N. Talaty, K. Datsenko, B.L. Wanner and R.G. Coooks, In vivo recognition of Bacillus subtilis by desorption electrospray ionization mass spectrometry (DESI-MS), Analyst 134 (2009) 838-841. https://doi.org/10.1039/b900069k

[6] P. Caputo, M.C. Di Martino, B. Perfetto, F. Iovino and G. Donnarumma, Use of MALDI-TOF MS to discriminate between biofilm-producer and non-producer strains of Staphylococcus epidermidis, Int. J. Environ. Res. Public Health 15 (2018) 1695. https://doi.org/10.3390/ijerph15081695

[7] A.M. Gaudreau, J. Labrie, C. Goetz, D. Dufour and M. Jacques, Evaluation of MALDI-TOF mass spectrometry for the identification of bacteria growing as biofilms, J. Microbiol. Methods 145 (2018) 79-81. https://doi.org/10.1016/j.mimet.2018.01.003

[8] A. Vertes, V. Hitchins and K.S. Phillips, Analytical challenges of microbial biofilms on medical devices, Anal. Chem. 84 (2012) 3858-3866. https://doi.org/10.1021/ac2029997

[9] J. Azeredo, N. F. Azevedo, R. Briandet, N. Cerca, T. Coenye, A. R. Costa, M. Desvaux, G. Di Bonaventura, M. Hébraud, Z. Jaglic, M. Kàcaniovà, S. Knøchel, A. Lourenço, F. Mergulhão, R. L. Meyer, G. Nychas, M. Simões, O. Tresse and C. Sternberg, Critical review on biofilm methods, Crit. Rev. Microbiol. 43 (2017) 313-351. https://dx.doi.org/10.1080/1040841X.2016.1208146

[10] M. Longo, S. Rioual, P. Talbot, F. Faÿ, C. Hellio and B. Lescop, A high sensitive microwave sensor to monitor bacterial and biofilm growth, Sens. Bio-Sens. Res. 36 (2022) 10049. https://doi.org/10.1016/j.sbsr.2022.100493

[11] H. Karimi-Maleh, F. Karimi, M. Alizadeh, A.L. Sanati, Electrochemical sensors, a bright future in the fabrication of portable kits in analytical systems, Chem. Rec. 20 (2020) 682-692. https://doi.org/10.1002/tcr.201900092

[12] W. Zhang, R. Wang, F. Luo, P. Wang and Z. Lin, Miniaturized electrochemical sensors and their point-of-care applications, Chin. Chem. Lett. 31 (2020) 589-600. https://doi.org/10.1016/j.cclet.2019.09.022

[13] L. Abi Nassif, S. Rioual, W. Farah, C. Hellio, M. Fauchon, R. Trepos, M. Abboud, E. Diler, D. Thierry, B. Lescop, Reduction of potential ennoblement of stainless steel in natural seawater by an ecofriendly biopolymer, J. Environ. Chem. Eng. 8 (2020) 103609. https://doi.org/10.1016/j.jece.2019.103609

[14] N. Poma, F. Vivaldi, A. Bonini, P. Savo, A. Kirchhain, Z. Ates, B. Mela, D. Bottai, A. Tavanti, F. Di Francesco, Microbial biofilm monitoring by electrochemical transduction methods, Tr. Anal. Chem. 134 (2021) 116134. https://doi.org/10.1016/j.trac.2020.116134

[15] A. Jayaraman, E.T. Cheng, J.C. Earthman and T.K. Wood, Anexic aerobic biofilms inhibit corrosion of SAE 1018 steel through oxygen depletion, Appl. Microbiol. Biotechnol. 48 (1997) 11-17. https://doi.org/10.1007/s002530051007.

[16] Y. Zhao, E. Zhou, Y. Liu, S. Liao, Z. Li, D. Xu, T. Zhang, T. Gu, Comparison of different electrochemical techniques for continuous monitoring of the microbiologically influenced corrosion of 2205 duplex stainless steel by marine Pseudomonas aeruginosa biofilm, Corros. Sci. 126 (2017) 142-151. https://doi.org/10.1016/j.corsci.2017.06.024.

[17] Y. Lekbach, Z. Li, D. Xua, S. El Abed, Y. Dong, D. Liu, T. Gu, S.I. Koraichi, K. Yang, F. W, Salvia officinalis extract mitigates the microbiologically influenced corrosion of 304L stainless steel by Pseudomonas aeruginosa biofilm, Bioelectrochemistry 123 (2019) 193-203. https://doi.org/10.1016/j.bioelechem.2019.04.006

[18] A.M. Giorgi-Pérez, A.M. Arboleda-Ordoñez, W. Villamizar-Suárez, M. Cardeñosa-Mendoza, R. Jaimes-Prada, B. Rincón-Orozco and M.E. Niño-Gómez, Biofilm formation and its effects on microbiologically influenced corrosion of carbon steel in oilfield injection water via electrochemical techniques and scanning electron microscopy, Bioelectrochemistry 141 (2021) 107868. https://doi.org/10.1016/j.bioelechem.2021.107868

[19] N. Poma, F. Vivaldi, A. Bonini, P. Salvo, B. Melai, D. Bottai, A. Tavanti and F. Di Francesco, A graphenic and potentiometric sensor for monitoring the growth of bacterial biofilms, Sens. Actuators B 323 (2020), 128662. https://doi.org/10.1016/j.snb.2020.128662

[20] D-G. Ha and G.A. O'Toole, c-di-GMP and its effects on biofilm formation and dispersion: a Pseudomonas aeruginosa review, Microbiol. Spectr. 3 (2015) 301-317. https://doi.org/10.1128/microbiolspec.MB-0003-2014

[21] T. Rasamiravaka, Q. Labtani, P. Duez and M. El Jaziri, The Formation of Biofilms by Pseudomonas aeruginosa: A review of the natural and synthetic compounds interfering with control mechanisms, BioMed Res. Int. (2015) 759348. https://doi.org/10.1155/2015/759348

[22] M.T.T. Thi, D. Wibowo and B.H.A. Rehm, Pseudomonas aeruginosa biofilms, Int. J. Mol. Sci. 21 (2020) 8671-8695. https://doi.org/10.3390/ijms21228671.

[23] P. Naves, G. del Prado, L. Huelves, M. Garcia, V. Ruiz, J. Blanco, V. Rodríguez-Cerrato, M.C. Ponte and F. Soriano, Measurement of biofilm formation by clinical isolates of Escherichia coli is method-dependent, J. Appl. Microbiol. 102 (2008) 585-590. https://doi.org/10.1111/j.1365-2672.2008.03791.x.

[24] X. Liu, J. Cai, H. Chen, Q. Zhong, Y. Hou, W. Chen, Antibacterial activity and mechanism of linalool against Pseudomonas aeruginosa, Microb. Pathog. 141 (2020) 103980. https://doi.org/10.1016/j.micpath.2020.103980.

[25] G. Wijesinghe, A. Dilhari, B. Gayani, N. Kottegoda, L. Samaranayake and M. Weerasekera, Influence of laboratory culture media on in vitro growth, adhesion, and biofilm formation of Pseudomonas aeruginosa and Staphylococcus aureus, Med. Princ. Pract. 18 (2019) 28-35. https://doi.org/10.1159/000494757

[26] P. Krishnaveni and V. Ganesh, Electron transfer studies of a conventional redox probe in human sweat and saliva bio-mimicking conditions, Sci. Rep. 11 (2021) 7663. https://doi.org/10.1038/s41598-021-86866-z

[27] T. Pajkossy, M.U. Ceblin and G. Mészáros, Dynamic electrochemical impedance spectroscopy for the charge transfer rate measurement of the ferro/ferricyanide redox couple on gold, J. Electroanal. Chem. 899 (2021) 115655. https://doi.org/10.1016/j.jelechem.2021.115655

[28] A. Baudler, I. Schmidt, M. Langner, A. Greiner and U. Schröder, Does it have to be carbon? Metal anodes in microbial fuel cells and related bioelectrochemical systems, Energy Environ. Sci. 8 (2015) 2048-2055. https://doi.org/10.1039/C5EE00866B

[29] A. J. Bard and L. R. Faulkner, Electrochemical Methods, 2nd Ed. (2001), J. Wiley & Sons.

[30] M. Maruthupandy, M. Anand, G. Maduraiveeran, A.S.H. Beevi and R.J. Priya, Electrical conductivity measurements of bacterial nanowires from Pseudomonas aeruginosa, Adv. Nat. Sci: Nanosci. Nanotechnol. 6 (2015) 045007. https://doi.org/10.1088/2043-6262/6/4/045007

[31] L. Liu, Y. Xu, F. Cui, Y. Xia, L. Chen., X. Mou. And J. Lv, Monitoring of bacteria biofilms forming process by in-situ impedimetric biosensor chip, Biosens. Bioelectron. 112 (2018) 86-92. https://doi.org/10.1016/j.bios.2018.04.019

[32] H. Ben-Yoav, A. Freeman, M. Sternheim and Y. Shacham-Diamand, An electrochemical impedance model for integrated bacterial biofilms, Electrochim. Acta 56 (2011) 7780–7786. https://doi.org/10.1016/j.electacta.2010.12.025

Figure 1

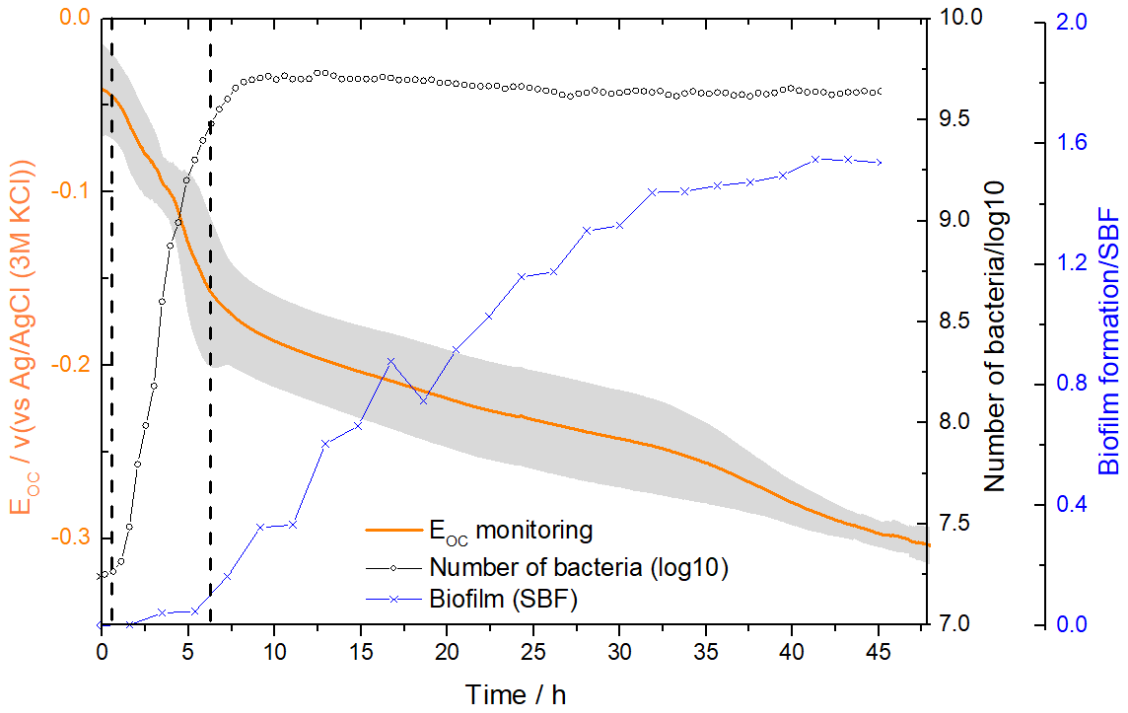

Fig. 1. Overlay of electrochemical monitoring (orange – left axis) with bacterial growth curve (black – first right axis) and biofilm formation curve (blue – second right axis) at $T = 37$ °C. The orange curve displays the mean of 4 measurements and the grey cloud represents the standard deviation. The dashed vertical lines represent the step boundaries as described in the text

Figure 2

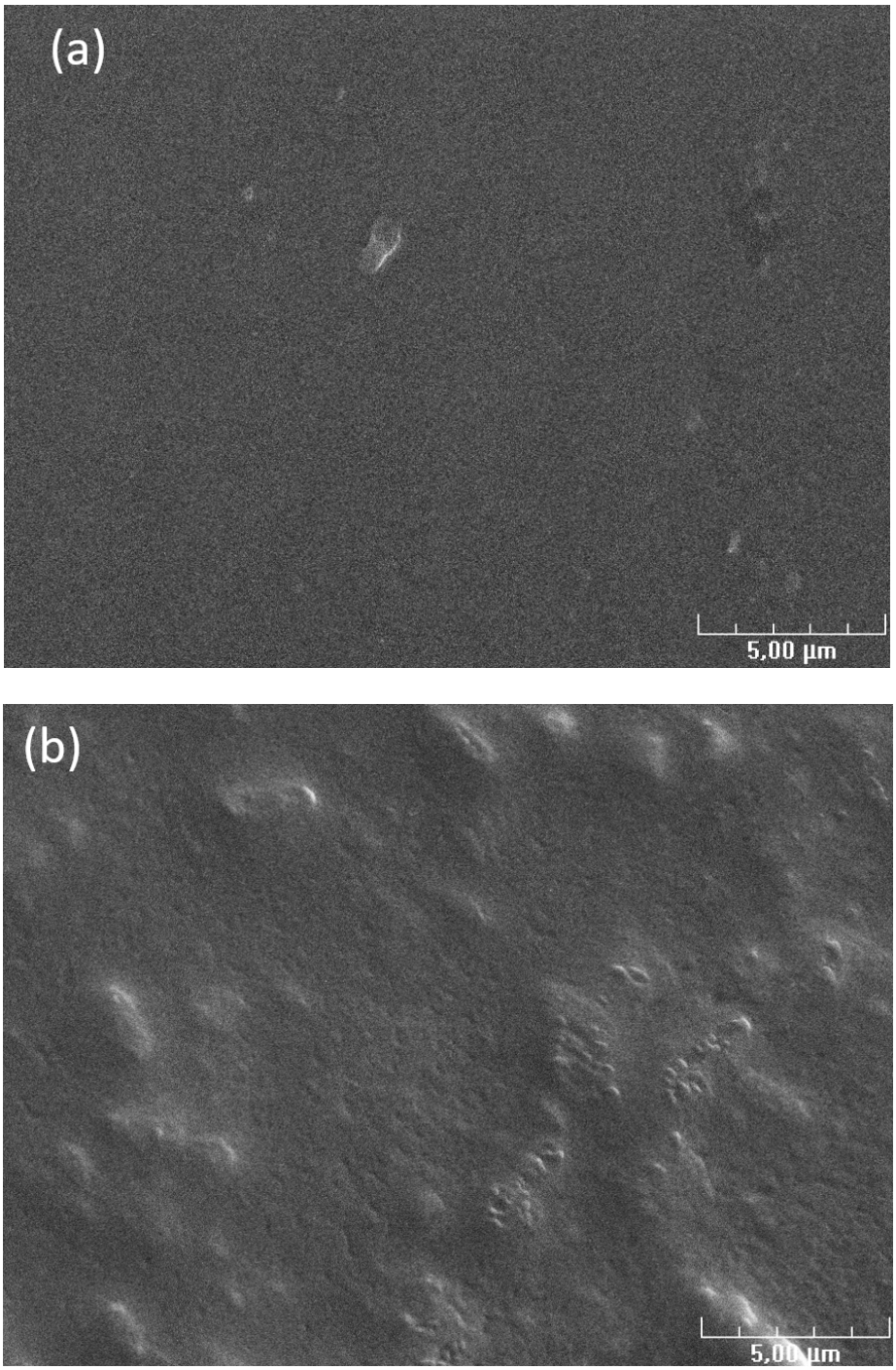

Fig. 2. SEM images of GC surface after immersion in inoculated TSB for 3 hours (a) and for 24 hours (b).

Figure 3

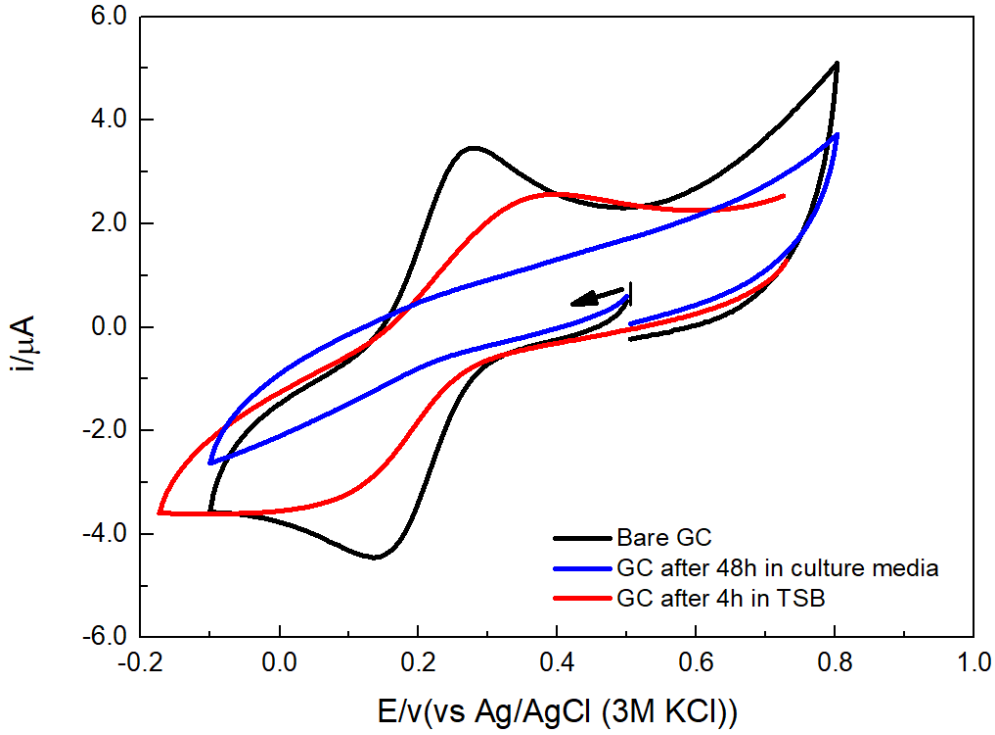

Fig. 3. Cyclic voltammetry of glassy carbon electrode in $[Fe(CN)_6]K_3$ (0.5 mM) / KCl (0.1 M) / H_2O solution for various conditions: V = 0.1 V.s^{-1}, T = 19 ± 2°C. The starting potential is indicated by a vertical line, with an arrow giving the scanning direction.

Figure 4

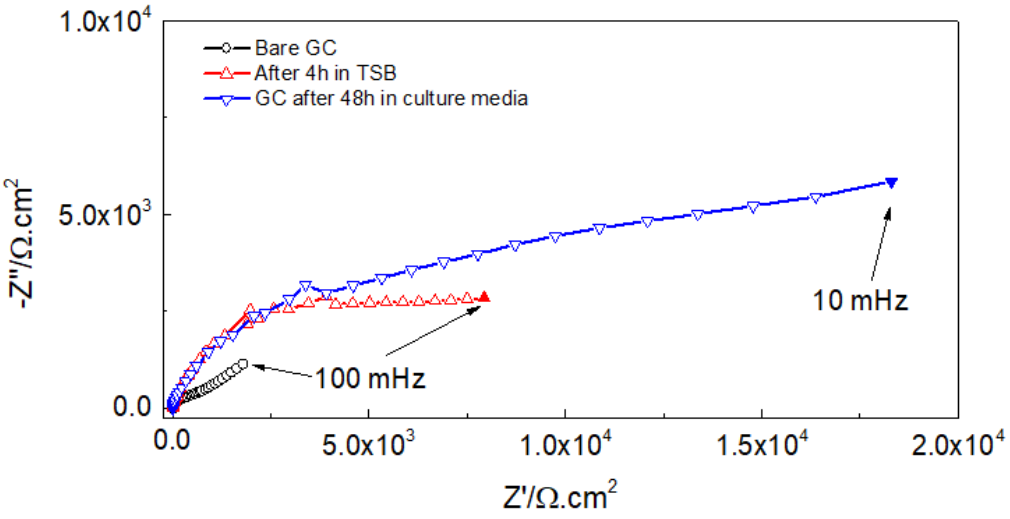

Fig. 4. Nyquist diagrams obtained with glassy carbon in $[Fe(CN)_6]K_3$ (0.5 mM) / KCl (0.1 M) / H_2O solution for various conditions.

Figure 5

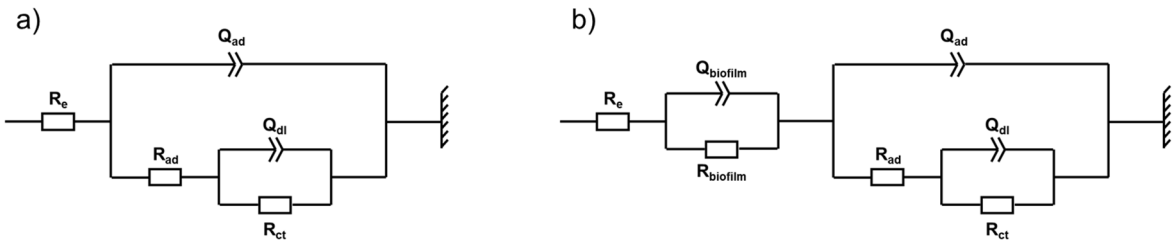

Fig. 5. Equivalent circuits proposed for systems without (a) and with (b) biofilm in TSB solution.

Schematic 1

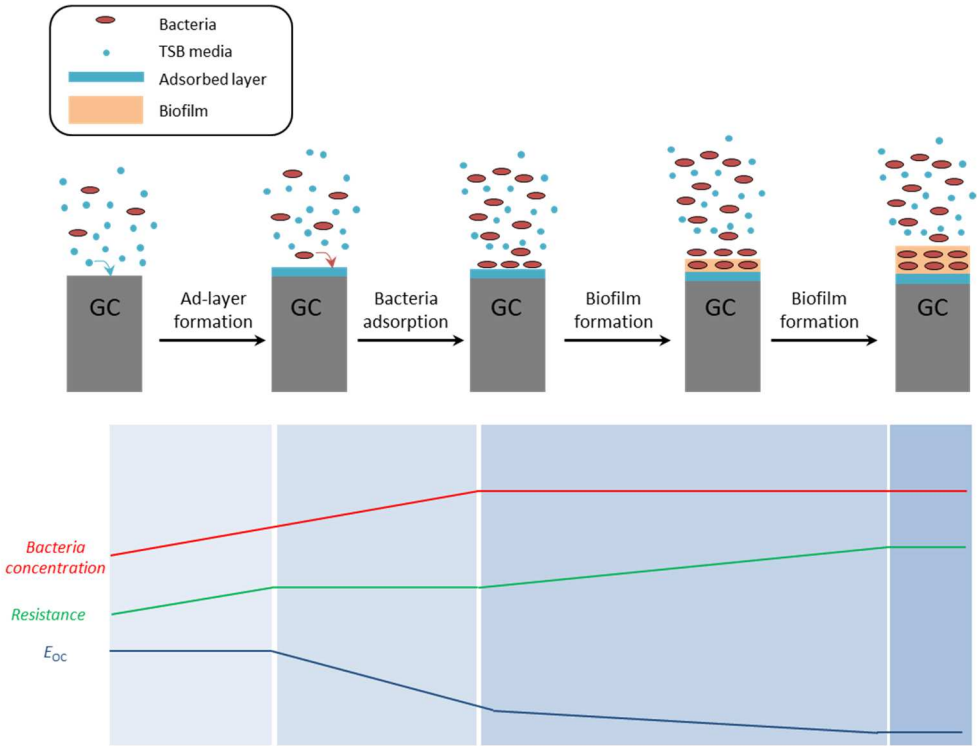

Schematic 1. Proposed chronological mechanism based on experimental data.